J. Great Lakes Res. 26(4):495–505
Internat. Assoc. Great Lakes Res., 2000

# NOTE

# Sediment Resuspension Near the Keweenaw Peninsula, Lake Superior During the Fall and Winter 1990–1991

**Nathan Hawley**

*Great Lakes Environmental Research Laboratory*
*2205 Commonwealth Boulevard*
*Ann Arbor, Michigan 48105*

***ABSTRACT.*** *During the winter of 1990–1991 time series measurements of current velocity, temperature, and attenuation (a measure of water transparency) were made at a site in 91 m of water near Copper Harbor, MI. The observations show that bottom resuspension occurred several times during the unstratified period. The resuspension is the result of the interaction between high bottom current velocities and surface waves generated by strong winds. Transport during the storms was almost entirely alongshore, although some offshore transport of material occurred. Calculations show that suspended material could have been transported eastward several hundred km during the unstratified period.*

***INDEX WORDS:*** *Lake Superior, sediment resuspension, sediment transport.*

## INTRODUCTION

The Keweenaw current is one of the most pronounced features of the circulation of Lake Superior. This coastal current flows along the north shore of the Keweenaw Peninsula (Fig. 1) with a net transport to the east. There is a general belief that the presence of the current enhances the alongshore and inhibits the cross-shelf movement of terrestrial inputs. The effects of the current are also seen on the lake floor, where side-scan sonar studies have shown numerous furrows oriented parallel to the prevailing flow (Flood 1989).

Several studies have investigated the dynamics of the current (see the references listed in Viekman and Wimbush, 1993), but almost all of these studies have been conducted during the summer when the lake is stratified. One exception is the study conducted by Viekman and his co-investigators who, as part of an investigation on the origin of bottom furrows, made time series measurements of the current velocity during the fall and winter of 1986–87. In October 1986 they deployed a single current meter located 10 meters above the bottom (mab),and two vertical profiling current meters at a site 2 km offshore of Copper Harbor, Michigan. Data from the profiling meters (which operated for about a month) were described by Viekman *et al.* (1989, 1992), who established the presence of secondary circulation over the bottom furrows. They suggested that the secondary circulation cells were active in maintaining the furrows by enhancing deposition rates at the furrow crests and retarding deposition in the furrow troughs. Flood (1989) described the data collected by the current meter moored 10 mab (which operated throughout the winter) and speculated that strong bottom currents during the winter flow parallel to the furrow orientation (which is parallel to the shore). Viekman and Wimbush (1993) extended the analysis of the velocity profiles to examine the vertical structure of the Keweenaw current during the unstratified period and found that the current acts primarily as a coastal jet that flows alongshore when the winds are strongly to the east. More recently two studies using remote sensing data have been conducted to determine the role of the current in transporting mine tailings (Van Luven *et al.* 1999, Budd *et al.* 1999). However no direct observations of sediment resuspension and transport have been reported. This note reports on some

*Corresponding author. E-mail: hawley@glerl.noaa.gov

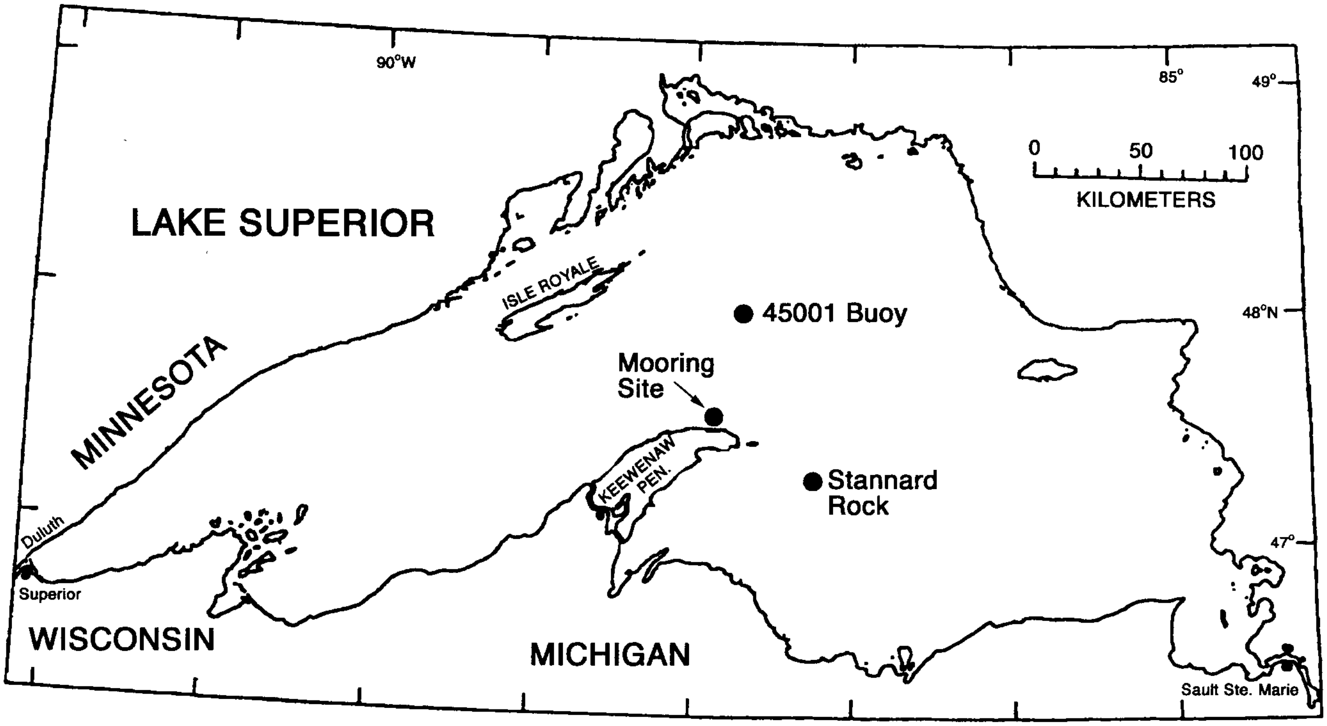


***FIG. 1. Location of the moorings, NOAA buoy 45001, and the meteorological station at Stannard Rock.***

observations of sediment resuspension made in the fall and winter of 1990–1991.

## METHODS

Two moorings were deployed on 22 Aug 1990 from the RV *Seward Johnson* about 1 km offshore of Copper Harbor, Michigan in 91 m of water (Fig. 1); details of the moorings are given in Table 1. The deployment sites are located near the tip of the Keweenaw Peninsula and at the eastern end of the furrow field described by Flood (1989). The moorings deployed by Viekman *et al.* (1989, 1992) were close to this site, but in slightly deeper water (100 m). Bathymetric contours in this area are essentially parallel to the shoreline (which runs east-west) to about 90 m. The lake deepens quickly to this depth (the 90 m contour is only about 1 km offshore), but farther offshore the slope lessens and the bathymetry becomes more irregular.

One mooring (47° 29.18′N, 87° 52.14′W) included two EG&G vector averaging current meters at 10 and 25 meters above the bottom (mab). These current meters recorded continuous 15 m averages of both current velocity and water temperature. The temperature measurements are accurate to 0.2°C while the current velocity measurements are accurate to 0.01 m/s with a lower threshold of 0.02 m/s. Both meters operated until they were retrieved in the summer of 1991, but neither record is continuous. The meter 10 mab failed between 15 September and 22 October 1990, and the meter 25 mab failed during several short intervals in January, March, and April 1991.

The second mooring (47° 29.14′N, 87° 52.28′W) included a bottom-resting tripod that supported three thermistors, four transmissometers, and a Marsh-McBirney 585 electromagnetic current meter. The bottom transmissometer was mounted horizontally on the tripod, but the other transmissometers were mounted vertically on the mooring line. The velocity measurements are accurate to 0.01 m/s, with a threshold of 0.005 m/s. The thermistors are accurate to 0.2°C. Water transparency was recorded to 0.001 volts over a nominal 5 volt range. The voltages were converted to beam attenuation (BAC) using

$$BAC = -\ln(V_w/V_A * V_F/5)/PL \quad (1)$$

Where $V_H$ is the voltage measured in water, $V_A$ is the voltage measured by the transmissometer in air,

***TABLE 1. Deployment data.***

| VACM data —22 August 1990–11 June 1991 | | | |
|---|---|---|---|
| Parameter | Height (mab) | Sample rate | Sample period |
| Temperature °C | 10,25 | Continuous | 15 minutes |
| Current velocity m/sec | 10,25 | Continuous | 15 minutes |

| Tripod data – August 22, 1990–January 9, 1991 | | | |
|---|---|---|---|
| Parameter | Height (mab) | Sample rate | Sample period |
| Temperature °C | 0.9,5,20 | 1 Hz | 1 min/hour |
| Attenuation (1/m) | 0.9,5,10,20 | 1 Hz | 1 min/hour |
| Current velocity m/sec | 0.5 | 1 Hz | 1 min/hour |

| Bottom sediment | |
|---|---|
| Size | % |
| Clay (< 0.004 mm) | 12.40% |
| Fine silt (0.004–0.002 mm) | 23.35% |
| Medium silt (0.002–0.004 mm) | 28.60% |
| Coarse silt (0.004–0.006mm) | 16.71% |
| Sand (> 0.006 mm) | 18.94% |

$V_F$ is the voltage measured in air at the factory, and PL is the pathlength of the transmissometer (in this case 0.25 m). Beam attenuation has the units of 1/m, and is a measure of the amount of material suspended in the water. The acoustic release on this mooring fired prematurely on 10 January 1991, and the tripod then moved about 0.5 km before being tipped on its side. Since there is no usable attenuation or velocity data from this mooring after 9 January, the data analysis is restricted to the period between 22 August 1990 and 9 January 1991.

Weather data and wave measurements (significant wave height and peak-energy wave period) were obtained from NOAA buoy 45001, which was moored approximately 60 km north of the study area. The buoy was retrieved for the winter on 2 December 1990 and not re-deployed until May 1991, so no wave observations are available after 2 December. Additional weather data (but no wave observations) were obtained from NOAA CMAN station STDM4 (which is maintained throughout the year) located at Stannard Rock, about 60 km southeast of the study area. Wind observations from the two sites are very similar, so only those from Stannard Rock are presented. Ice cover data obtained from the Navy/NOAA Joint Ice center shows that there was little ice cover in the area prior to mid-January.

One vertical profile of temperature and water transparency was made near the deployment site using a Sea Tech transmissometer (0.25 m path length) and a Yellow Springs thermistor. Pressure readings were made with a Varian pressure sensor. The accuracy of the thermistor and transmissometer are the same as those used for the time series measurements; the depth readings are accurate to 0.5 m.

Bottom samples were collected from within 5 m of the tripod by a submersible (the *Johnson Sea-Link II*) carried by the *Seward Johnson*. Four punch cores 0.2 m long and 0.05 m in diameter were collected by the submersible and returned intact to the surface. The material in the top 10 mm was used to measure the particle size distribution. The material was first wet-sieved using a 60 mm screen to remove the sand-sized material. The fine fraction was analyzed using a Spectrex model ILI-1000 particle counter and the coarser material with a settling tube. Results of the analysis are given in Table 1; all of the sand-sized material is either fine (0.25 to 0.125 mm) or very fine (0.125 to 0.062 mm) sand. The results agree with those made by Flood (1989) who described the bottom material as a “sandy-muddy silt.” Observations made from the submersible showed that the bottom at both sites was essentially flat with no traces of small-scale bed forms. Occasional feeding traces were observed. The bottom material is cohesive, but was easily resuspended by the *Sea-Link II*.

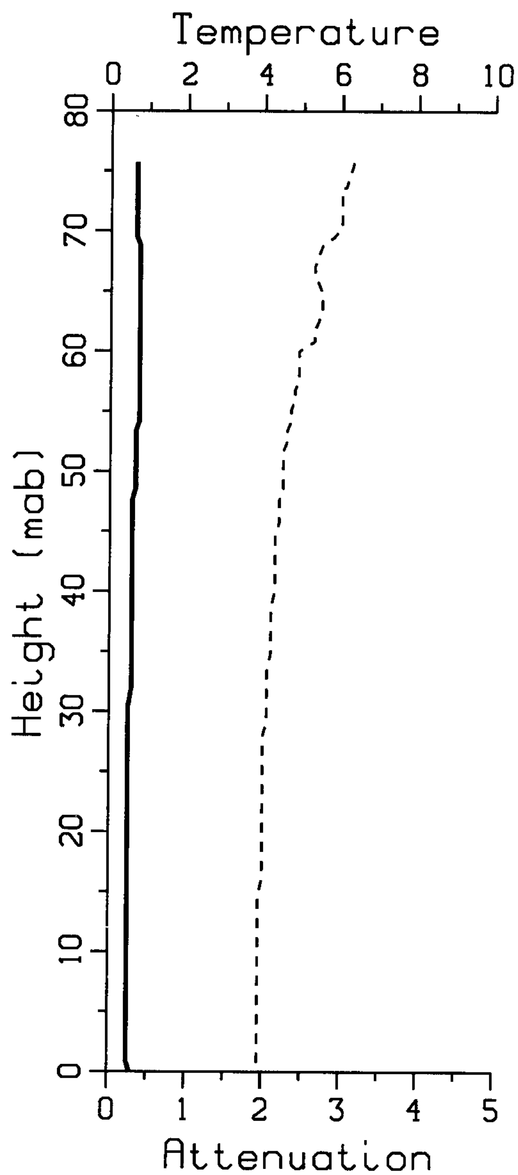


***FIG. 2. Vertical profile of attenuation (solid line, 1/m) and water temperature (dashed line, °C) made at a station close to the deployment site on 22 August 1990.***

## RESULTS

The vertical profile made on 22 August (Fig. 2) shows that the beam attenuation was very low from top to bottom. There is no evidence of a benthic nepheloid layer except within 1 m of the bottom, and even there it is very poorly developed. Although about half the temperature decrease occurred in the top 15 m, there is no evidence of a well-developed thermocline. The surface water temperature was significantly less than at the NOAA buoy (10°C)—this may indicate that an upwelling event was in progress. Winds during the 2 days prior to the deployment were from the northeast, which would induce upwelling (Niebauer *et al.* 1978).

Wind speeds (Fig. 3) were fairly low at the beginning of the deployment, but were quite strong after mid-September. Maximum wind speeds of over 20 m/s were recorded on 18 October, and there were numerous instances when the speed exceeded 15 m/s. The strong winds generated large waves on several occasions (Fig. 4). The largest observed waves occurred on 18 October, when the wave height was over 5 m and the wave period was 9 s. Waves almost as large occurred on 22 November, when the height was 4.3 m and the period was 10 s. There are no wave measurements available after 2 December and no wave hindcasts are available for this year, but since the winds were no stronger than those in November it seems unlikely that the waves were significantly larger than those observed in November—except possibly in late December and early January when the combination of strong winds from the northwest (15 m/s) and a long fetch may have produced larger waves.

At the beginning of the deployment the surface water temperature at the buoy was considerably higher than the other temperatures (Fig. 4), but three storms in September and October caused the thermocline to break down and vertical mixing to occur. By 20 October the water column was essentially isothermal, and during November the surface water cooled more rapidly than the water at depth. The resulting instability caused the usual fall overturn of the lake so that by early December the water column was again isothermal. The water then cooled until it reached 0°C at the end of January (not shown).

Eleven storms (identified from the current velocity records) occurred during the deployment (Table 2, Figs. 3 and 4). Current speeds were low until the end of September when the first (storm 1, 22–27 September) of the three storms responsible for the breakdown of the thermocline occurred. Of these three storms the second (storm 2, 3–8 October) was the most intense; current speeds reached 0.43 m/s 25 mab and 0.14 m/s 0.5 mab (the 10 mab current meter was not operating during these storms). Although the surface waves were largest during storm 3 (16–19 October), the current speeds were less than during storms 1 and 2. Current direction (Fig.

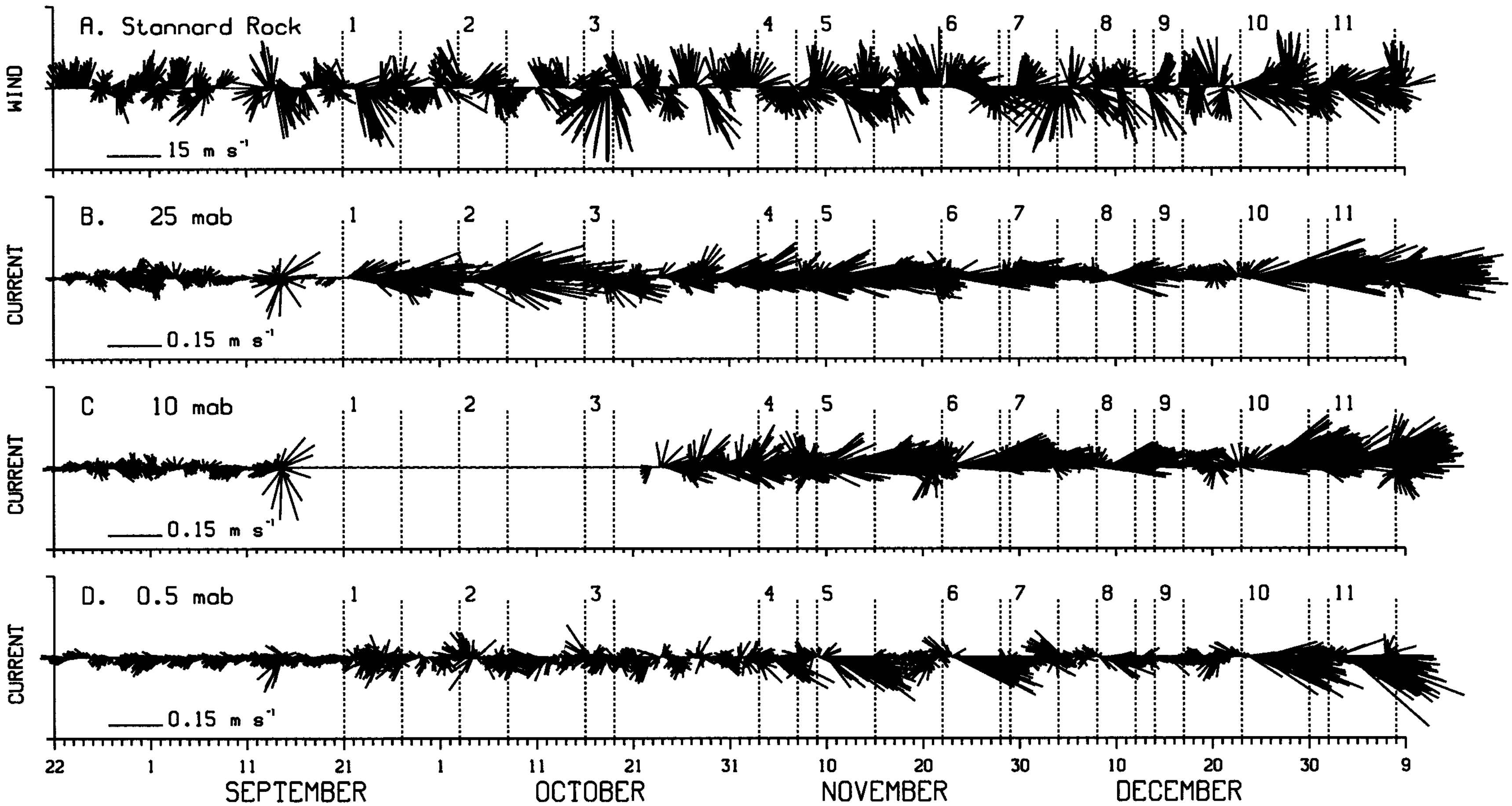


*FIG. 3. Stickplots of the wind and current velocities. The dashed vertical lines show the beginning and end of the eleven storms listed in Table 2. A. Wind velocity at Stannard Rock. The oceanographic convention is used, so the wind on 18 October is from north to south. B. Current velocity 25 mab. C. Current velocity 10 mab. The current meter did not work between 15 September and 22 October. D. Current velocity at 0.5 mab.*

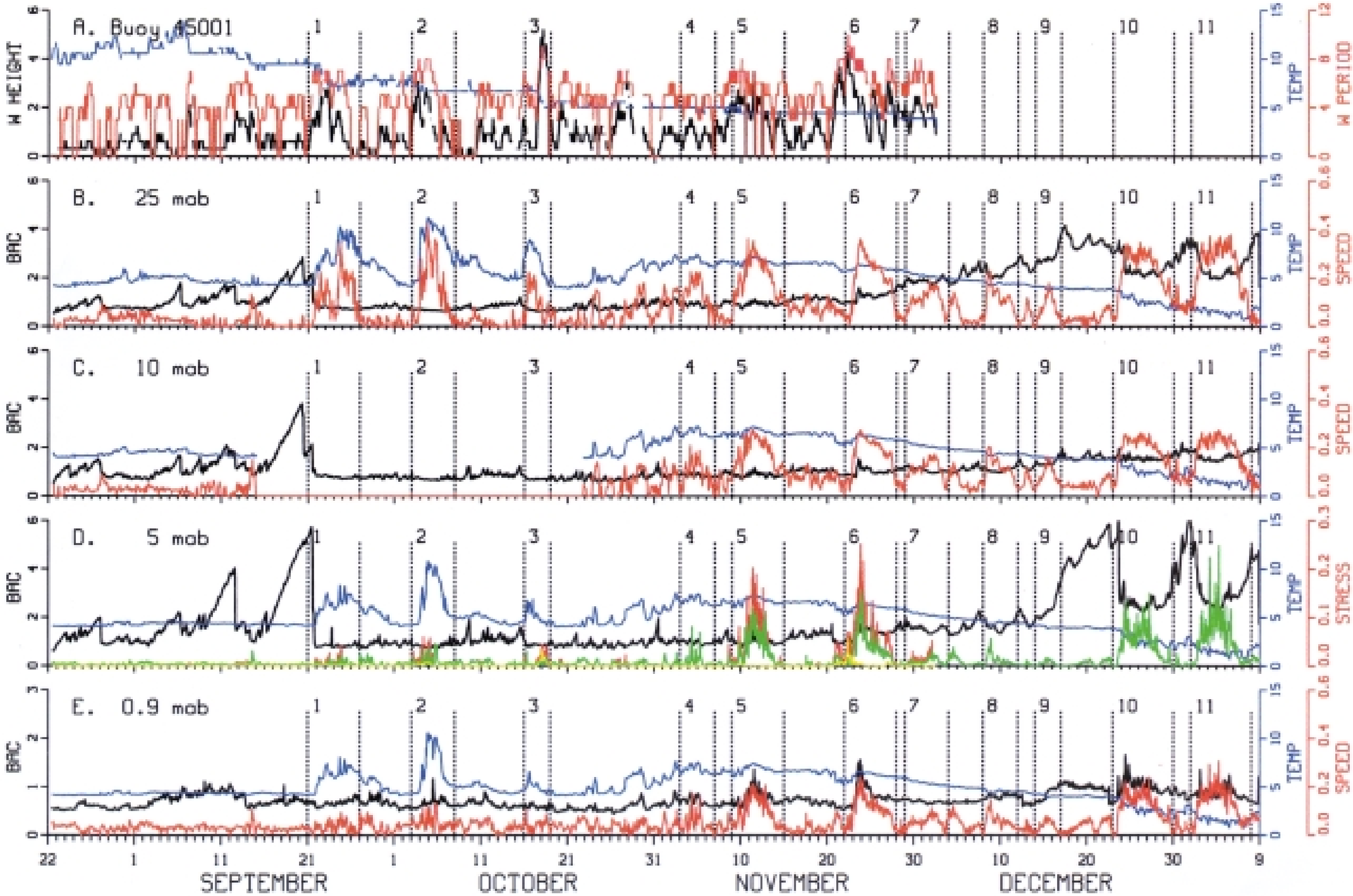


*FIG. 4. Time series observations. The color of the lines are the same as the appropriate vertical axis. Attenuation (BAC) has the units of 1/m, current speed is in m/s, and temperature in °C. The dashed vertical lines show the beginning and end of the eleven storms listed in Table 2. A. Observations at NOAA buoy 45001. Wave height is in meters and wave period in seconds. B. Observations at 25 mab. Attenuation measurements were made at 20 mab. C. Observations at 10 mab. D. Observations at 5 mab. The bottom stress due to combined waves and currents is shown in red, the bottom stress due to current action alone in green, and the bottom stress due to wave action alone in yellow. E. Observations at 0.9 mab (attenuation and temperature) and at 0.5 mab (current speed). Note that the attenuation scale is not the same as in the other panels.*

***TABLE 2. Storm conditions.***

| Storm # | Dates | Current Direction | Maximum Combined Stress ($N/m^2$) | Wave Stress ($N/m^2$) | Current Stress ($N/m^2$) | Resuspension? |
|---|---|---|---|---|---|---|
| 1 | Sept 21–27 | Varies | 0.04 | 0.00 | 0.03 | No |
| 2 | Oct 3–8 | Varies | 0.06 | 0.00 | 0.03 | No |
| 3 | Oct 16–19 | East | 0.04 | 0.04 | 0.00 | No |
| 4 | Nov 3–7 | East | 0.08 | 0.00 | 0.08 | No |
| 5 | Nov 9–15 | East | 0.14* | 0.00* | 0.09* | Yes |
| | | | 0.20 | 0.00 | 0.12 | |
| 6 | Nov 22–28 | East | 0.07* | 0.01* | 0.02* | Yes |
| | | | 0.25 | 0.00 | 0.15 | |
| 7 | Nov 29–Dec 4 | East, Northwest | 0.05 | 0.00 | 0.03 | No |
| 8 | Dec 8–12 | East | — | — | 0.06 | No |
| 9 | Dec 14–17 | East | — | — | 0.02 | No |
| 10 | Dec 23–30 | East | — | — | 0.02* | Yes |
| | | | | | 0.15 | |
| 11 | Jan 1–8 | East | — | — | 0.05* | Maybe |
| | | | | | 0.22 | |
| | | | | | 0.09* | |

* indicates values at which resuspension began
Values of current and wave stresses are those at the time of the maximum combined stress. Stress values of less than 0.005 $N/m^2$ are reported as 0.00.

3) during the three storms was primarily alongshore to the east at 25 mab but showed considerable variability near the bottom.

Eight other major storms occurred during the remainder of the deployment. Although the speeds at 25 mab are similar to those during the first three storms, the bottom speeds are considerably greater. During the four largest storms (storm 5, 9–15 November; storm 6, 22–28 November; storm 10, 23–30 December; and storm 11, 1–8 January), bottom current speeds exceeded 0.2 m/s, with a maximum value of 0.31 m/s on 3 January. Current velocities during all of these storms were primarily alongshore to the east at all elevations, but the direction usually has an onshore component near the bottom and an offshore component at the upper elevations (bottom contours run essentially east-west at the deployment site). Bottom currents were offshore at the end of storm 7, but otherwise the only times when the bottom current had an offshore component was between storms.

Figure 4D also shows the bottom stress due to combined wave and current action, current action alone, and wave action alone. Only the current stress is shown after 2 December since no wave data are available. The combined stress was calculated using the model of Lou *et al.* (2000) and the wave stress from linear wave theory. The bottom current stress, $t_c$, was calculated from

$$\tau_c = \rho\, u_*^2 \qquad (2)$$

where $\rho$ is the density of water and $u_*$ is the bottom shear velocity. Equation 3 was used to calculate $u_*$

$$u_z/u_* = 1/\kappa \ln(z/z_0) \qquad (3)$$

where $u_z$ is the current velocity at height z above the bottom (0.5 m) and $\kappa$ is von Karman's constant (0.4). The precise value of the surface roughness ($z_0$) is difficult to determine, but the absence of bed forms and the small grain size means that the boundary is hydraulically smooth. Luettich *et al.* (1990) suggested that in this case $z_0$ equals 0.2 mm, so that value has been used to calculate $u_*$. The calculations show that the current stresses were considerably larger than the wave stresses throughout almost the entire deployment (storm 3 is an exception), but wave action did enhance the combined bottom stress during most of the storms.

Interpretation of the transparency records is complicated by the fouling that occurred on the top three sensors. The large attenuations observed at 5, 10, and 20 mab prior to 22 Sept are most likely due to material settling on the lens of the transmissometers (recall that these three units were mounted vertically). The strong currents on 22 Sept appear to have removed this material, but fouling began again after storm 7 (during storm 6 at 25 mab), and continued through the remainder of the observation period. After storm 6 there is also a slight increase in the bottom attenuation between storms. This may be due to fouling, or it may indicate that the ambient suspended sediment concentration increased after that storm.

The attenuation record from 0.9 mab shows that large attenuation increases occurred during storms 5, 6, and 10, and smaller increases during storm 11. Some indication of increased attenuation during storms 5 and 6 can also be seen in the 5, 10, and 20 mab attenuation records, but the variations are no larger than many other variations in these records.

Figure 5 shows the observations during storm 6. The increase in attenuation at 9:00 on 23 November can be clearly seen at all four elevations. This increase continues until early on 25 Nov when the attenuation returns to background levels (although the background level is higher than prior to the storm, as noted above). The simultaneous increase in attenuation and combined bottom stress indicates that the increase in attenuation is due to local resuspension and not lateral advection, as does the fact that the bottom current direction is slightly onshore (if material had been resuspended at shallower depths and then advected to the site, the bottom currents would need to have an offshore component). However the data also show that bottom resuspension did not occur until 9:00 on 23 November (when the estimated combined stress was only 0.07 N/m$^2$) even though the estimated combined bottom stress was higher at both 6:00 and 12:00 (greater than 0.1 N/m$^2$ in both cases). This is probably due to differences in wave conditions at the buoy from those at the deployment site. If the waves at the deployment site were larger at 9:00, then the combined stress would have been larger.

Although the observations show that bottom resuspension occurred either three or four times during the deployment, the changes in attenuation are much smaller than those reported from shallower depths in Lake Michigan (Lesht and Hawley 1987, Lee and Hawley 1998, Hawley and Lee 1999). This probably is caused by a combination of less intense hydrodynamic activity due to the greater water depth (which reduces the influence of surface wave action—surface wave action was more important in the Lake Michigan studies) and a limited amount of sediment available for resuspension.

## DISCUSSION

Although the stress due to current action was the primary cause of sediment resuspension, surface wave action enhanced the bottom stress during most of the storms. Winds were from the west (where the fetch is greatest) during storms 10 and 11, so the waves during these storms were probably at least as large as those during storms 5 and 6, and may have been larger. The only wave model results for Lake Superior are those reported by Driver *et al.* (1992), who reported the results of a 31-year (1956 to 1987) wave hindcast study. Although their calculations do not cover the deployment period, their findings at a station near the deployment site (station 36, 47° 31.80′N, 87° 55.80′W) indicate that waves larger than those observed during the deployment occurred very rarely (only 13 occurrences out of over 90,000 calculations). The hindcasts also show many more instances (about 150) with similar wind conditions when the waves were no larger than those observed. Surface waves may have been larger during storms 10 and 11, but since there is no proof of that, it seems best to assume that they were approximately the size of those observed during storm 6. This means that the combined bottom stresses during these storms would be similar to those observed during storms 5 and 6.

The combined bottom stress did not exceed 0.07 N/m$^2$ during the seven storms when resuspension did not occur, so an initial estimate of the minimum stress required for erosion is 0.08 N/m$^2$. Resuspension occurred during storm 5 at a bottom stress of 0.14 N/m$^2$, but during storm 6 the bottom stress was only 0.07 N/m$^2$ when resuspension began. However the actual stress during storm 6 may have been higher if the wave conditions were slightly different, and since the bottom stress exceeded 0.1 N/m$^2$ both shortly before and after resuspension began, a value of 0.1 N/m$^2$ seems to be a reasonable estimate of the minimum shear stress required for erosion. This is in reasonable agreement with both the value of Miller *et al*. (1977) for the critical shear velocity needed to resuspend sediment of this size (0.007 m/s$^1$, which is equivalent to a stress of 0.05 N/m$^2$), and with the experimental results of MacIntyre *et al.* (1990), who found no resuspension of cohesive sediments at a stress of 0.1 N/m$^2$, but did observe erosion at 0.2 N/m$^2$.

Although the bottom current meter failed during

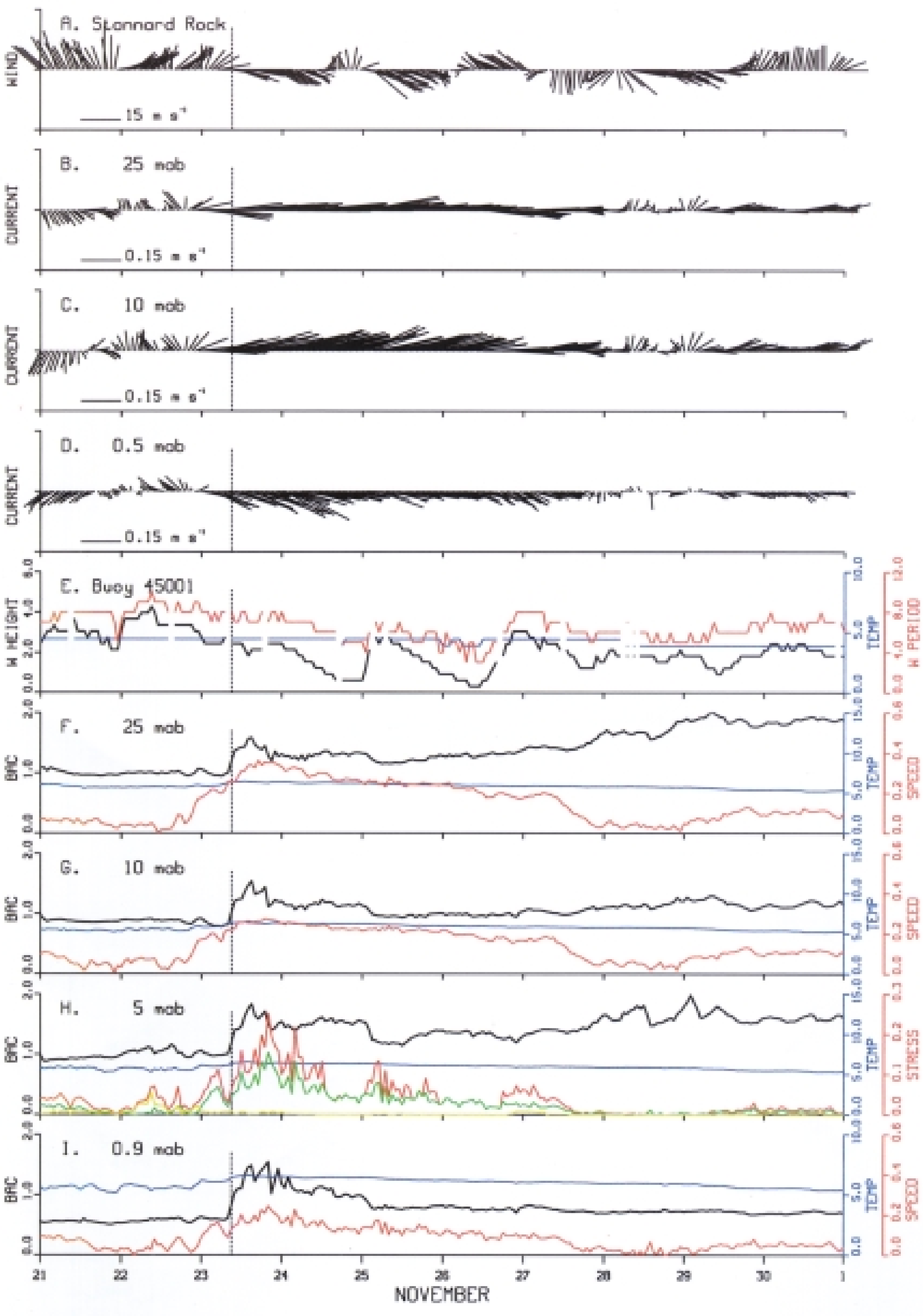


***FIG. 5.** Observations during storm 6. The vertical line indicates when resuspension began. The color of the lines are the same as the appropriate vertical axis in panels E-I. Attenuation (BAC) has the units of 1/m, current speed is in m/s, and temperature in °C. A. Wind velocity at Stannard Rock. B. Current velocity at 25 mab. C. Current velocity at 10 mab. D. Current velocity at 0.5 mab. E. Observations at NOAA buoy 45001. Wave height is in meters and wave period in seconds. F. Observations at 25 mab. Attenuation measurements were made at 20 mab. G. Observations at 10 mab. H. Observations at 5 mab. The bottom stress due to combined waves and currents is shown in red, the stress due to current action alone in green, and the stress due to wave action alone in yellow. I. Observations at 0.9 mab (attenuation and temperature) and at 0.5 mab (current speed).*

early January, the measurements made at 10 and 25 mab continued until June 1991. These show that during storms 5, 6, 10, and 11, the current speeds exceeded 0.25 m/s at 10 mab. An examination of the current speeds for the entire deployment period shows that these values were exceeded four other times during the deployment – two more times in January and once each in February and April. Strong winds also occurred frequently during the remainder of the deployment, so it seems likely that waves as large as those observed during storm 6 also occurred. Thus it is possible that bottom resuspension occurred 4 more times during the unstratified period. The lack of any events between mid-February and late April is probably due to the extensive ice cover that formed in the lake that winter. However the number of events may vary substantially from winter to winter. During the winter of 1986–87 for instance, Flood's (1989) data show that the 10 mab current speed exceeded 0.25 m/s only once.

Although it is risky to extrapolate from data collected at a single site, if the conditions observed here are typical of those that occur along the entire Keweenaw Peninsula, then an estimate of the material transport during the winter can be made. The net alongshore transport at 0.5 mab during the periods of elevated attenuation in storms 5, 6, and 10 is 25, 33, and 36 km respectively, so a conservative estimate of the net transport during the winter is over 240 km (eight storms times 30 km/storm). At the upper elevations the transport rates are even greater—approximately 50 km/storm at 10 mab and 60 km/storm at 25 mab (based on the same time periods used for the 0.5 mab calculations). Since the entire Keweenaw Peninsula is only about 150 km long, this means that material resuspended at a depth of 90 m could have been transported the entire length of the peninsula during one winter. During the winter of 1986–87, however, the transport would have been much less. Resuspension occurs more frequently at shallower sites, so if the current speeds are similar the transport of suspended material could be much greater. For larger particles, of course, the transport will be less than that calculated here, since they will not remain in suspension for as long a period.

Cross-shelf transport was much less than the alongshore transport. Transport near the bottom during the three storms was onshore near the bottom, but was slightly offshore at the upper elevations (about 8 km/storm at 10 mab and 3 km/storm at 25 mab). Although these values must be used with caution (since they are very sensitive to the exact alignment of the shoreline), it is possible that sediment suspended at least 10 mab was transported to the deeper parts of the lake during the storms. What is clear is that the alongshore transport is considerably greater than the cross-shelf transport. Thus these calculations support the general belief that the Keweenaw current enhances alongshore transport and inhibits cross-shelf movement of terrestrial inputs.

## CONCLUSIONS

The observations show that bottom resuspension occurred several times during the winter of 1990–91 at a water depth of 91 m. The resuspension events were caused by a combination of high bottom current speeds and surface waves generated by high (15 to 20 m/s) wind speeds. Resuspension occurred only during the unstratified period, when the winds were stronger and the lack of a thermocline permitted increased near-bottom velocities. Transport of resuspended material is primarily alongshore during the storms. Offshore movement occurred primarily during the intervals between storms near the bottom, but did occur to a limited extent during the storms at 10 and 25 mab. Transport calculations suggest that material could have been transported in suspension several hundreds of kilometers to the east during a single winter.

## ACKNOWLEDGMENTS

Ship time on the RV *Seward Johnson* and the undersea vehicle *Johnson Sea-Link II* was provided by the NOAA National Undersea Research Program at Avery Point, CT. Dr. Larry Sanford made several valuable suggestions on an earlier version of the manuscript. The comments of two anonymous reviewers significantly improved the manuscript. This is GLERL contribution #1178.

## REFERENCES

Budd, J., Kerfoot, W.C., Pilant, A., and Jipping, L.M. 1999. The Keweenaw current and ice rafting: use of satellite imagery to investigate copper-rich particle dispersal. *J. Great Lakes Res.* 25:642–661.

Driver, D.B., Reinhard, R.D., and Hubertz, J.M. 1992. *Hindcast wave information for the Great Lakes: Lake Superior*. United States Army Corps of Engineers Waterways Experiment Station, Vicksburg, MS. Wave Information Study Report 23.

Flood, R.D. 1989. Submersible studies of current-modified bottom topography in Lake Superior. *J. Great Lakes Res.* 15:3–14.

Hawley, N., and Lee, C.-H. 1999. Sediment resuspension and transport in Lake Michigan during the unstratified period. *Sedimentology* 46:791–805.

Lee, C.-H., and Hawley, N. 1998. The response of suspended particulate material to upwelling and downwelling events in southern Lake Michigan. *J. Sedimentary Res.* 68:819–831.

Lesht, B.M., and Hawley, N. 1987. Near-bottom currents and suspended sediment concentration in southeastern Lake Michigan. *J. Great Lakes Res.* 13:375–386.

Lou, J., Schwab, D. J., Beletsky, D., and Hawley, N. 2000. A model of sediment resuspension and transport dynamics in southern Lake Michigan. *J. Geophys. Res.* 105:6591–6610.

Luettich, R. A. Jr., Harleman, D. R. F., and Somlyódy, L. 1990. Dynamic behavior of suspended sediment concentrations in a shallow lake perturbed by episodic wind events. *Limnol. Oceanogr.* 35:1050–1067.

MacIntyre, S., Lick, W., and Tsai, C. H. 1990. Variablity of entrainment of cohesive sediments in freshwater. *Biogeochem.* 9:187–200.

Miller, M.C., McCave, I.N., and Komar, P.C., 1977, threshold of sediment motion under unidirectional currents. *Sedimentology* 24:507–527.

Niebauer, H.J., Green, T., and Ragotzkie, R.A. 1978. Coastal upwelling/downwelling cycles in southern Lake Superior. *J. Phys. Oceanog.* 7:918–927.

Van Luven, D.M., Huntoon, J.E., and Maclean, A.L. 1999. Determination of the influence of wind on the Keweenaw Current in the Lake Superior basin as identified by Advanced Very High Resolution Radiometer (AVHRR) imagery. *J. Great Lakes Res.* 25:625–641.

Viekman, B.E., and Wimbush, M. 1993. Observations of the vertical structure of the Keweenaw current, Lake Superior. *J. Great Lakes Res.* 19:470–479.

______, Wimbush, M., and Van Leer, J.C. 1989. Secondary circulations in the bottom boundary layer over sedimentary furrows. *J. Geophys. Res.* 94: 9721–9730.

______, Flood, R.D., Wimbush, M., Faghri, M., Asako, Y., and Van Leer, J.C. 1992. Sedimentary furrow and organized flow structure: a study in Lake Superior. *Limnolol. Oceanogr.* 37:797–812.

*Submitted: 29 May 2000*
*Accepted: 7 September 2000*
*Editorial handling: Barry M. Lesht*